GEOACTA **43(1):**1-16 (2018) ISSN 1852-7744
© 2019 Asociación Argentina de Geofísicos y Geodestas

ANNUAL VARIABILITY OF SEA SURFACE TEMPERATURE IN THE NORTHERN ARGENTINEAN CONTINENTAL SHELF

VARIABILIDAD ANUAL DE LA TEMPERATURA SUPERFICIAL DEL MAR EN LA PLATAFORMA CONTINENTAL ARGENTINA NORTE

Moira Luz Clara[1,2,3], Claudia G. Simionato[3,4], Andrés J. Jaureguizar[5,6,7]

1 Consejo Nacional de Investigaciones Científicas y Técnicas (CONICET), Moreno 3527 piso 3, B7600GIA, Mar del Plata, Buenos Aires, Argentina.
2 Instituto Nacional de Investigación y Desarrollo Pesquero (INIDEP), Paseo Victoria Ocampo Nº 1, Escollera Norte, B7602HSA, Mar del Plata, Buenos Aires, Argentina.
3 Instituto Franco-Argentino para el Estudio del Clima y sus Impactos (UMI-IFAECI/CNRS), Intendente Güiraldes 2160, Ciudad Universitaria, Pabellón II, piso 2, C1428EGA, Ciudad Autónoma de Buenos Aires, Argentina.
4 Departamento de Ciencias de la Atmósfera y los Océanos (FCEN-UBA) and Centro de Investigaciones del Mar y la Atmósfera (CONICET-UBA), Intendente Güiraldes 2160, Ciudad Universitaria, Pabellón II, piso 2, C1428EGA, Ciudad Autónoma de Buenos Aires, Argentina.
5 Comisión de Investigaciones Científicas de la Provincia de Buenos Aires (CIC), Calle 526 e/10 y 11, CP1900, La Plata, Buenos Aires, Argentina.
6 Instituto Argentino de Oceanografía, CC 804, Florida 8000 (Camino La Carrindanga km 7,5), Bahía Blanca, Buenos Aires, Argentina
7 Universidad Provincial del Sudoeste (UPSO)-subsede Coronel Pringles, Sáenz Peña 867, Coronel Pringles CP 7530, Buenos Aires, Argentina

ABSTRACT

Twelve years of daily satellite data (0.1° spatial resolution) were used to study the seasonal variability of the sea surface temperature (SST) over the Northern Argentinean Continental Shelf (NACS; between 33°- 45° S and 52°- 66° W). The seasonal cycle, which includes the annual and semi-annual signals, was assessed using harmonic analysis. The annual cycle explained more than 90% of the total variance in the NACS, with SST amplitudes varying from 3.4 to 7.6° C. Largest variances values for this timescale were observed along the Argentinean coast and the inner shelf; particularly in the El Rincón region (exceeding 96%). Empirical Orthogonal Function Analysis (EOF) in S-Mode was applied to daily SST anomalies in the annual timescale, indicating that nearly 94% of its variance was explained by the first two modes, which accounted for 70 and 24% of the variance, respectively. Mode 1 prevailed most of the year with its positive phase occurring in autumn/winter and the negative in spring/summer. This mode revealed the seasonal radiative warming/cooling, related to the heating/cooling in summer/winter in most of the NACS; the shallow waters of the Río de la Plata and El Rincón were heated and cooled more and faster than deeper waters. The weakest seasonal heating/cooling occurred around Península Valdés, where vertical mixing maximizes due to tidal action. Mode 2 corresponded to early spring and early fall in their positive and negative phases, respectively. This mode was related to a transition during the early intermediate seasons when the cooling/heating of an extended coastal region connecting Península Valdés and the Río de la Plata occur.

Keywords: SST seasonal cycle, EOF analysis, water regime areas, Southwestern Atlantic Ocean.

RESUMEN

La variabilidad estacional de la temperatura superficial del mar (TSM) en la Plataforma Continental Argentina Norte (PCAN, entre 33º- 45º S y 52º- 66º O) fue estudiada a partir de doce años de datos satelitales de resolución diaria y 0,1° de resolución espacial. El ciclo estacional, que incluye las señales anuales y semianuales, fue evaluado mediante análisis armónico. El ciclo anual explicó más del 90% de la varianza total en la PCAN, con amplitudes de TSM que variaron entre 3,4 y 7,6 ºC. Los mayores valores de varianza para esta escala temporal se observaron a lo largo de la costa argentina y la plataforma continental interna, particularmente en la región de El Rincón (excediendo el 96%). Un análisis de funciones ortogonales empíricas (EOFs) en modo-S aplicado a las anomalías diarias de TSM en la escala anual indicó que casi el 94% de la varianza fue explicada por los primeros dos modos, que representaron el 70 y el 24% de la varianza, respectivamente. El Modo 1 prevaleció la mayor parte del año con su fase positiva en otoño/invierno y la negativa en primavera/verano. Este modo reveló el calentamiento/enfriamiento radiativo estacional, relacionado con el aumento/disminución de las temperaturas en verano/invierno en gran parte de la PCAN; las aguas poco profundas del Río de la Plata y El Rincón se calientan/enfrían más y más rápido que las aguas más profundas. El calentamiento/enfriamiento estacional más débil se produjo alrededor de Península Valdés, donde la mezcla vertical por acción de las mareas es intensa. El Modo 2 corresponde a principios de primavera y principios de otoño en sus fases positiva y negativa, respectivamente. Este modo se encontró relacionado con una transición durante el inicio de las temporadas intermedias, cuando se produce el enfriamiento/calentamiento de una larga región costera que conecta Península Valdés y el Río de la Plata.

Palabras Clave: Ciclo estacional de la temperatura superficial del mar, análisis EOF, zonas de regímenes de agua, Océano Atlántico Sudoccidental.

INTRODUCTION

The ocean has influence on a range of processes, from daily weather events to global climate variability. One accessible indicator of the ocean's state and potential influence is the sea surface temperature (SST). SST is important in climatic studies and air-sea interaction processes. The knowledge of SST variability is essential to study not only the global climate changes on inter-annual and decadal timescales (*e.g.*, El Niño and La Niña events) but also the shorter timescale oceanic processes, such as frontal dynamics, upwelling and downwelling events, and eddy and plume evolution (Wang et al., 2004), as well as in biological applications. In general, SST variability is dominated by the annual cycle in most of the global ocean. This cycle is a pattern that nearly repeats itself every 12 months and can mask low-frequency climatic trends, which include the monthly means and the quarterly cycle. The knowledge of the SST cycles leads to a better understanding of the timing of biological events, since SST is a good indicator for the water column stratification in the Southwestern Atlantic Ocean (SWAO) (Podestá et al., 1991).

The dominant SST annual cycle forcing is the change of the distribution of incoming solar radiation along the year due to the orbit of the Earth around the Sun and the tilt of the Earth axis rotation. The exchange of energy between the sea surface and the atmosphere is one of the energy sources for the atmospheric circulation. Trenberth and Stepaniak (2004) provide a quantification of the seasonal uptake and release of heat by the oceans that substantially moderate the climate in maritime regions. These authors affirm that the solar radiation is absorbed and stored within the ocean, so that maximum SSTs tend to occur at the end of the summer in the extra tropics. Kara et al. (2009), based in atmospherically forced ocean general circulation model simulations, under the assumption that variations in the climatologic monthly SSTs are driven by atmospheric variables, demonstrate that shortwave radiation is the most influential variable controlling the seasonal cycle of SST over 34.3% of the global ocean whereas wind speed is the second most important variable (27.2%).

In this work the seasonal cycle over the Northern Argentinean Continental Shelf (NACS, between 33°- 45° S and 52°- 66° W) was studied utilizing almost 12 years of satellite data. This cycle was defined as the expected evolution of the climatic variable through the year (Yashayaev and Zveryaev, 2001). This approach involves the parametric description of the seasonal cycle, which is defined by a small number of parameters: harmonic coefficients,

annual and semi-annual amplitudes and phases, etc. Thus, the annual and semi-annual harmonics form the dominant part of the seasonal cycle. This method allows the determination of the appropriate climatic value for any moment of a year and avoids the misinterpretation of natural seasons because of the wrong setting of fixed calendar months. Thereby, the production of the winter and summer fields is based on the actual extremes, as defined from the phase analysis. The parametric description of the seasonal cycle is more accurate than the use of monthly means because it considers a potential irregular distribution of observations throughout the year. The distribution of amplitudes and phases helps to disclose the origin of the seasonal cycle in different areas and to reveal the mechanisms responsible for the modification of its structure. The characteristics of the seasonal cycle can also be used to initialize oceanic and atmospheric models and may serve as a reference for validation of model simulations (*e.g.,* Giese and Carton, 1994) providing a firm criterion of model viability.

The annual pattern of SST variability in different portions of the SWAO Continental Shelf (Fig. 1) has been studied by other authors using diverse approaches and data. These previous studies, that use satellite images for different periods of time with different temporal and spatial resolutions (daily, 1984-1988 and 100 km (Podestá et al., 1991); weekly, 1982-1994 and 4 km (Lentini et al., 2000); monthly, 1985-2002 and 9 km (Rivas, 2010); daily, 2002-2008 and 11 km (Simionato et al., 2010); monthly, 2002-2011 and 1 km (Delgado et al., 2014)) and different spatial coverage (SWAO, NACS, Río de la Plata and El Rincón scales) indicate that, in general, SST in the NACS shows a marked seasonal cycle, with amplitudes decreasing offshore and southward, and with higher values in the shallow areas of the upper and intermediate Río de la Plata estuary and very coastal areas of El Rincón.

Thus, several regions of the Argentinean shelf were described regarding of the extent of the SST. However, a study showing how the SST at the different oceanographic areas (or systems) of the NACS respond both spatially and temporally on annual timescales as a whole and eventually co-vary is still missing. Therefore, this investigation aims to determine the SST spatial differentiation over the whole NACS concerning the seasonal cycle and try to reveal the forcing mechanisms of its spatial structure besides complementing and updating the knowledge of the SST at the spatial scale.

Study Area

The NACS (Fig.1) is located in the South Atlantic Ocean between 33°- 45° S and 52°- 66° W. This shelf comprises a variety of water masses mostly dominated by three large basins (San Matías Gulf, Río de la Plata and El Rincón) and influenced by Brazil and Malvinas marine currents (Guerrero and Piola, 1997). The Río de la Plata is one of the largest estuaries of the world (Shiklomanov, 1998), ranking fourth and fifth worldwide in freshwater discharge and drainage area, respectively (Framiñan et al., 1999). The San Matías Gulf (SMG) is a semi-enclosed basin and a very deep area on the NACS (Fig. 1). Bathymetry and local thermohaline characteristics force a semi-permanent gyre within the Gulf (Piola and Scasso, 1988). Shelf waters enter through the southeastern section of the mouth and are eventually exported through the northern section of the mouth (Piola and Scasso, 1988). Scasso and Piola (1988) present SMG as a warm and saline anomaly throughout the year, showing that it has a salinity maximum relative to the open shelf waters due to an excess of evaporation over precipitation of around 100 $cm \cdot yr^{-1}$, which is favored by the relatively higher sea surface temperatures found within the gulf.

The main oceanographic systems present in the NACS exhibit important differences in their spatial cover scale, magnitude forcing (river freshwater flow, tides, shelf currents, topography) and exhibit strong seasonal variations in its extension related to wind variability (Delgado et al., 2014; Lucas et al., 2005; Meccia et al., 2009; Palma et al., 2004a; Rivas, 2010; Simionato et al., 2001). During autumn and winter, the prevailing winds blow from the southwest, so that the waters of the Río de la Plata (RDP) and the SMG tend to discharge northeastward, and the El Rincón (ER) system extends its coverage along the coast. In spring and summer, the prevailing winds in the northern shelf blow from the northeast (Simionato et al., 2005). The drainage waters of RDP during these seasons are lower than in winter, with a dominant path to the south and towards the continental slope. The signal of SMG waters, also weaker, mainly extends eastward accompanying an increase in the Río Negro runoff. There are at least two sources of energy available in abundance in the area that may be important in maintaining the circulation in SMG and its vicinity: the wind intensity, that does not present significant seasonal variations and, therefore, neither would the associated circulation, and the tides, which occur at times of

the year in which there is a well-developed thermocline (Piola and Scasso, 1988). The SMG region is characterized by large tidal amplitudes (Glorioso and Flather, 1997; Palma et al., 2004b; Moreira et al., 2011), intense westerly winds, particularly in winter (Palma et al., 2004a), and significant surface heat and freshwater fluxes (Scasso and Piola, 1988; Rivas and Beier, 1990). In particular, the Península Valdés frontal system (PVF) is one of the best-known tidal fronts in the NACS, located south of the SMG entrance (Carreto et al., 1986; Glorioso, 1987; Bava et al., 2002; Glorioso, 1987; Bianchi et al., 2005, 2009; Derisio et al., 2014).

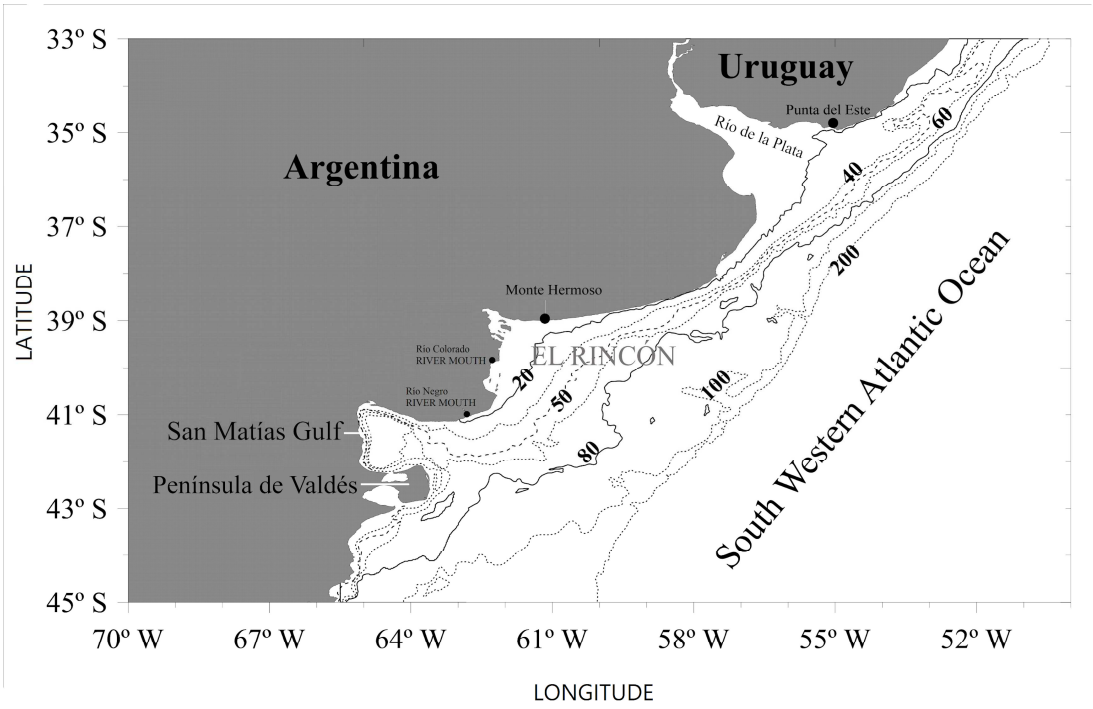

Figure 1. Northern Argentinean Continental Shelf (study area) showing the principal geographical references and isobaths.
Figura 1. Plataforma Continental Argentina Norte (área de estudio) y principales referencias geográficas y batimétricas.

The signal observed in the coastal waters and the ER is different; it is stronger and detected to the north of approximately 38°50' S (Guerrero, 1998; Lucas et al., 2005; Piola and Rivas, 1997). In this area, spring and summer mean physical distributions lead to conjecture that stratification increases because of increased insolation, reduced winds and subsurface intrusions into the shelf (Martos and Piccolo, 1988).

The NACS is characterized by a gentle slope and low relief features (Parker et al., 1997). The continental shelf widens from north to south, and it is characterized by a mean north–northeastward surface flow in the middle shelf and a flow seasonally influenced in the inner shelf (Palma et al., 2008). This shelf comprises a variety of water masses: coastal waters and the so-called High Salinity Coastal Water, with relative salinity maximums (S> 34.0). This leads to the presence of several oceanic fronts (Guerrero and Piola, 1997; Acha et al., 2004). Waters dominated by the SMG, RDP and ER are separated from the mid and outer-shelf waters seasonally stratified by a thermal front called Middle Shelf Front (MSF). This front can be detected in SST horizontal distributions and can be visualized throughout the year, spanning between 38° S and 42° S between the 30 m and 80 m isobaths (Lucas et al., 2005; Martos and Piccolo, 1988; Saraceno et al., 2004).

The NACS is highly productive and diverse, with socio-economic relevance in the different systems and strongly related to dominant environmental conditions. Although the primary production in the main coastal shelf system is greater than the biomass supported by the system (Lercary et al., 2018, in press), its production is enhanced by the fertilization of continental freshwater discharge contributed by three principal rivers (RDP, Colorado and

Negro) and the Lagoa dos Patos, Brazil, (Lat -31° 04' S, Lon -51° 28' W, not shown in figure 1) (Garcia and Garcia, 2008; Lutz et al., 2010) and exhibit a clear seasonal pattern strongly related to changes in vertical stability, which controls nutrients and light availability (Carreto et al., 1995). Therefore, the availability of adequate food (high presence of phytoplankton and zooplankton) and the variation in the retention mechanisms (marine fronts, anticyclone gyres, oceanic circulation) will affect the successful fish larval recruitment and growth (Militelli, 2007; Rivas and Pisoni, 2010). Likewise, this oceanographic mechanism, together with the temperature and salinity distribution, affect the spatial arrangement of the principal fish assemblage (Menni et al., 2010), the species abundance and its population structure at different biological level (Elisio et al., 2017; Jaureguizar et al., 2016). The spatial and temporal variation in the environmental pattern affect the fishery landing (De Wysiecki et al., 2017) within the NACS, and thus, the improvement of the knowledge of patterns of environmental variables is significant for a fishery sustainable management within an ecosystem approach.

DATA AND METHODS

We used daily satellite SST data called "Blended Sea Surface Temperature" from the NOAA CoastWatch Program (NOAA NESDIS Office of Satellite Data Processing and Distribution, and NASA's Goddard Space Flight Center, OceanColor Web; https://coastwatch.pfeg.noaa.gov/infog/BA_ssta_las.html). This ocean product is derived from observations of both infrared and microwave remote sensors installed on multiple platforms, with 0.1° spatial resolution and daily temporal resolution over the period July 2002 - March 2014. Data are mapped into a regular grid of 0.1° × 0.1° and, through simply arithmetic, daily compositions over a 5-day period averages are produced.

This blended SST data set is one of the highest resolutions analyzed SST products that have been lately produced; it is estimated by optimal interpolation methods merging SST satellite coming from infrared and microwave sensors. The data processing is described in Powell et al. (2008). Combining the diverse sources of data makes possible to take advantage of each sensor's strengths (the high accuracy and resolution of the thermal infrared SST measurements and the better temporal and spatial coverage of passive microwave SST measurements). Merged or "Blended" products, in addition, have the advantage of having a low total error compared with the individual errors for each instrument. As shown in Reynolds et al. (2002), those errors can be dramatically reduced with blended products. In areas where data are scarce, as it is the case in the NACS, those blended products provide an opportunity of evaluating SST variability even on relatively short timescales. However, the problem of the blending is not free of difficulties; for instance, thermal infrared retrievals are measuring the skin temperature while passive microwave retrievals measure the sub-skin temperature. Wick et al. (2004) discussed the use of this combined data and concluded that it creates a new global, high quality, multi-sensor SST product at a fine spatial and temporal resolution that is global and regularly distributed, useful for climate modelers and scientists to better understand oceanic and atmospheric circulation patterns.

Taking advantage of the temporal resolution of our data (July 2002 - March 2014), we can apply a more accurate definition of the seasonal cycle than the use of monthly means, and more sophisticated statistical techniques to aid on the understanding of the involved processes.

Statistical Methods

The seasonal cycle of the SST daily anomalies respect to annual mean at every grid point (SSTA, hereafter) was computed by adjusting minimum squares sinusoidal functions (harmonic analysis).

To explore the co-variability of SSTA at different locations, *i.e.,* how SST variations at one location are related to those at another, alternative analyses methods could be applied. One commonly used approach is Principal Components based on Empirical Orthogonal Functions (EOF) analysis and extensions thereof (von Storch and Zwiers, 1999; Hannachi, 2004). Conceptually, EOF analysis determines a spatial pattern of variability that accounts for the maximum covariance between the SST anomaly timeseries at all the grid points in the dataset. This covariance maximum is extracted as the "first variability mode", or first or leading EOF. Then, the remaining co-variability is subject to the same decomposition with the added constraint that the second EOF pattern is orthogonal (*i.e.*, uncorrelated) in space to the leading

EOF pattern. This procedure is repeated until all *n* EOF patterns have been computed, where *n* is equal to the number of grid points. In practice, only the first few leading modes are robust as a result of the orthogonality constraint. EOF rotation may be used to circumvent this constraint; however, it may also result in patterns that are overly localized in space. Each EOF pattern is associated to a principal component (PC, *i.e.*, the corresponding timeseries or scores) that describes the temporal evolution of the covariance between the EOF pattern (in our case it would be a spatial pattern) and the SSTA field analyzed. The PC may be obtained by projecting (as a matrix product) the EOF pattern onto the original SST anomaly field at each time step to find the sign and amplitude of the pattern at every time (Deser et al., 2010). It should be noted that the sign of the EOF is arbitrary; however, the product of the EOF and the PC timeseries recovers the correct polarity of the mode at any given grid point and time. Although useful, EOF analysis is not infallible. The EOF modes depend on the spatial domain considered, are subject to orthogonality constraints, and may not be separable if they account for similar percentages of the total variance (North et al., 1982). Also, EOFs are empirically determined "modes" and thus are not necessarily equivalent to the dynamical modes of the system. It is always prudent to confirm EOF patterns with other techniques such as compositing, one-point correlation maps, linear regression analysis, etc.

Therefore, EOF analysis (S-Mode) over the fields of SSTA data was applied. To reflect the strength and physical robustness of every mode found, "composite" maps for the SSTA were computed, considering the positive and negative events identified with those days when high score values (>0.7 or <-0.7) were found.

RESULTS

The SST annual cycle accounted for over 90% of the total variance in all the study area; the most significant variances were observed along the inner shelf between 35° and 42° S (Fig. 2a). Particularly, in ER region values exceeded 96%. The lowest values were located along the RDP northern coast and at the outer continental shelf close to the shelf break.

The annual mean SST ranged from 10.5 to 20 °C (Fig. 2b), with a marked tilt of the isotherms from southwest to northeast, approximately following the regional isobathic features (Fig. 1). The lowest mean SST values were observed to the south of the continental shelf at depths higher than 100 m, whereas the highest values were found at the shallow upper RDP, where the continental runoff has considerable influence, and along the northern Uruguayan coast. A relatively low temperature cell, also observed by other authors (Glorioso, 1987; Pisoni et al., 2015; Rivas, 2010), was distinguished offshore PVF, due to this is a tidal front area where homogeneous and stratified waters meet and force the vertical mixing.

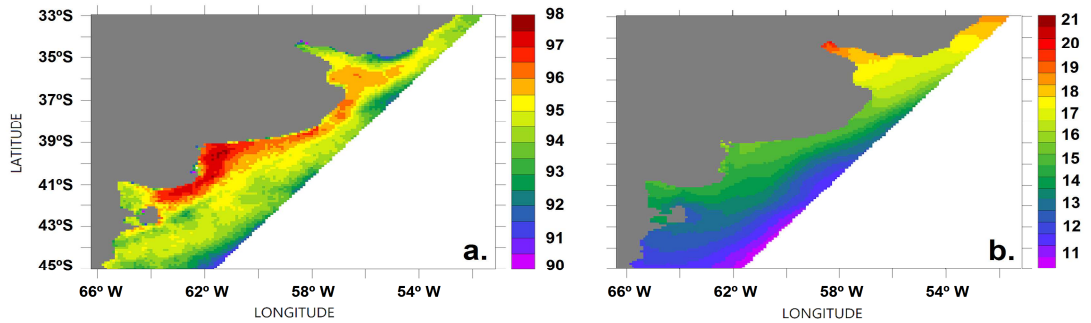

Figure 2. Spatial distribution of SST variance (%) in the Northern Argentinean Continental Shelf. SST annual cycle (a.) explains over 90%. Annual mean SST (b.) isotherms show a tilt from southwest to northeast. Note that the scale of every figure is different.

Figura 2. Distribución espacial de la varianza de TSM (%) en la Plataforma Continental Argentina Norte. El ciclo anual de TSM (a.) explica más del 90%. El campo medio anual de TSM (b.) muestra una inclinación de las isobaras de sudoeste a noreste. Notar que la escala de colores en cada figura es diferente.

The amplitude and phase of the annual cycle (Fig. 3a and b) showed similar spatial patterns, decreasing offshore north of 41º S and showing an opposite behavior in the vicinity of PVF, where minimum values are present close to the coast. The amplitude in the whole area ranged between 3.4 and 7.6 °C. The highest amplitudes occurred over the shallow areas (depths < 20 m) of the ER and the RDP, with a variation of over 6.8 °C between the warm and cold seasons (red areas in Fig. 3a). The lowest amplitudes were observed in the SMG with an extension from the PVF to the northeast, between the 50 and 80 m isobaths. Here, there were changes of up to 4.6 °C between the warm and the cold seasons (blue areas in Fig. 3a). The annual cycle phase (Fig. 3b) ranged between 28 and 72 days. There was a difference of about 30 days in the occurrence of the maximum/minimum SST seasonal anomaly between the outer shelf and the coastal systems of the Southwestern Atlantic Ocean. The shallower areas of the RDP and ER heat/cold, up to the end of the summer/winter, 40 days after than the PVF region. Thus, three shelf areas can be differentiated regarding their annual harmonic constants: the shallow areas of the ER and RDP, a region influenced by the PVF deep water, and the intermediate area of MSF and the Uruguayan coast.

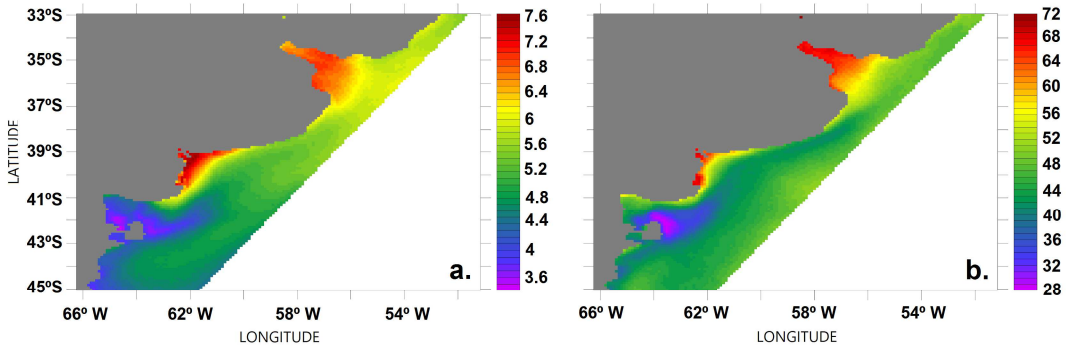

.

Figure 3. Amplitude (a.) and phase (b.) of SST annual cycle in Northern Argentinean Continental Shelf. The values of amplitude are in °C. The phase is defined as a time span (in days) between the beginning of the timeseries analyzed (July 27th) and the first cycle's minimum. The annual cycle phase ranged between 28 days around PVF and 72 days in shallow areas.

Figura 3. Amplitud (a.) y fase (b.) del ciclo anual de TSM en la Plataforma Continental Argentina Norte. Los valores de amplitud están expresados en °C. La fase es definida como el tiempo transcurrido (en días) entre el inicio de la serie temporal analizada (27 de julio) y el primer mínimo del ciclo. La fase del ciclo anual tiene un rango entre 28 días alrededor de FPV y 72 días en las áreas poco profundas.

The monthly mean SST fields computed from the adjusted annual cycle (Fig. 4) showed, for every month, a gradient pointing in the northwest direction (onshore). In January and February, the shallow regions of the NACS showed the highest temperatures, reaching around 26 °C in the RDP and around 23 °C in ER, whereas the coldest areas were in the southern shelf and at the SMG mouth, with approximately 14 °C. The areas close to the continental shelf break cooled first during March and April, but shallow areas rapidly get the same SST cool range during May to August, reaching 8/10 °C in the ER and middle coastal region, and about 10 °C in the RDP. During spring and early summer (September-December), shallow waters heat faster than the shelf and deeper areas and, therefore, the SST gradient points onshore again.

The EOF analysis applied to the SSTA (Fig. 5) indicated that nearly 94% of the annual variance was explained by the first two modes, which account for 70% (resembling the annual cycle pattern) and 24% (resembling the semi-annual cycle) of the variance, respectively. The spatial structure of Mode 1, *i.e.* the annual signal fields or EOFs (Fig. 5b), showed a pattern in which shallow areas (RDP and ER) heat/cool differently than deeper regions (SMG and PVF), as can be seen by the alternate factor loading sign. The PC timeseries of Mode 1 (Fig. 5a) showed minimum score values (<-0.7, negative phase) in late spring and summer of the Southern Hemisphere (end of October to March), whereas maximum values (>0.7, positive phase) occurred in late autumn and winter (May to early September).

The spatial pattern, or EOFs, of Mode 2 (Fig. 5d) showed a SSTA gradient pointing offshore/onshore at the inner ER and RDP with maximum values related to fall/spring; at the shelf region, between the 20 and 80 m isobaths and north of 42.5° S, maximum

positive/negative SSTA related to fall/spring season were observed. The PC timeseries of Mode 2 (Fig. 5c) showed minimum values (<-0.7, negative phase) in spring (September to October) and maximum values (>0.7, positive phase) in autumn (March to May).

.

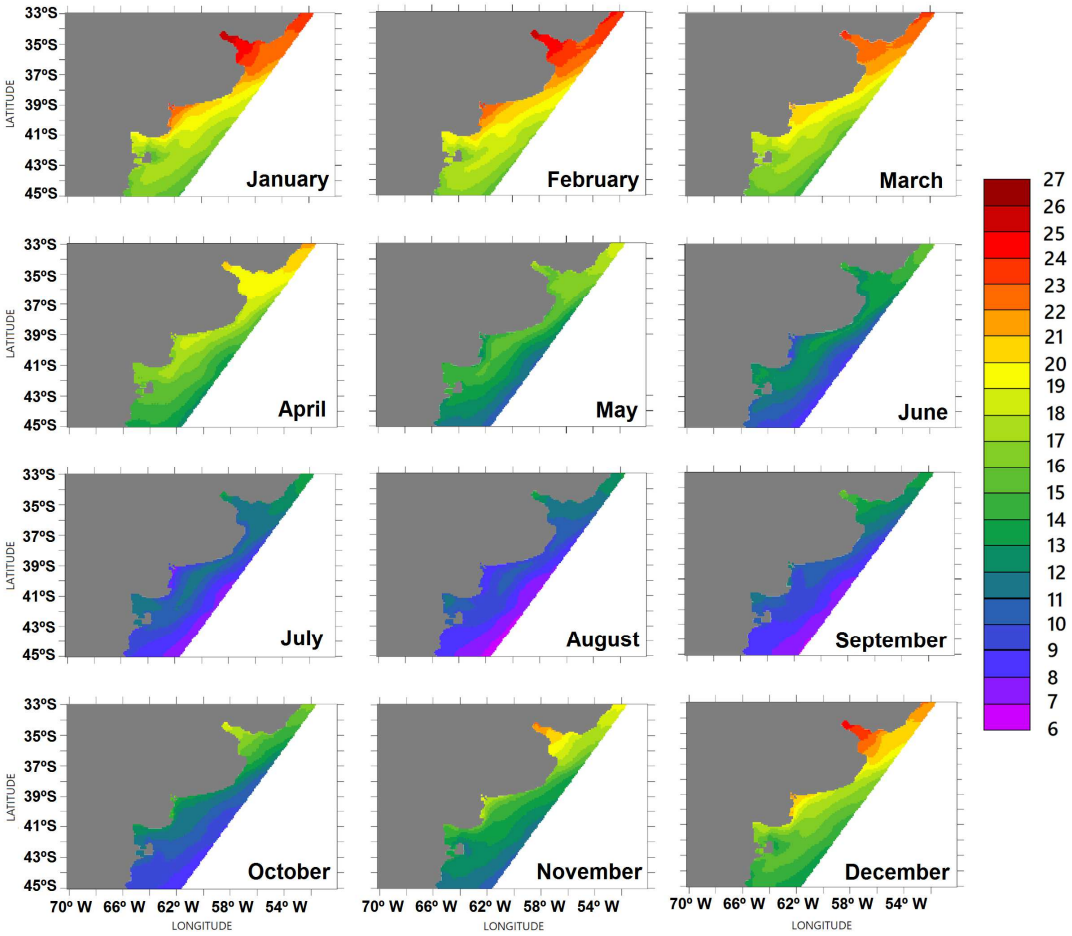

Figure 4. SST (°C) monthly mean distribution associated with the seasonal cycle in the Northern Argentinean Continental Shelf. Minimum SSTs occur in August and maximum SSTs in February.
Figura 4. Distribución de TSM media mensual (°C) asociada con el ciclo estacional en la Plataforma Continental Argentina Norte. Los mínimos valores de TSM se observan en agosto y los máximos en febrero.

To assess the robustness and better understand the meaning of the EOF modes, the SST composites for score values above/below +0.7/-0.7 were mapped (Fig. 6). The positive phase of Mode 1 occurred in autumn/winter (Fig. 6a), during 130 days of the year, whereas its negative phase occurred in spring/summer (Fig. 6b), during 151 days of the year. This mode very much resembled the structures of the annual cycle amplitudes and phases (Fig. 3) and reveals the seasonal warming/cooling associated with the radiative cycle. In winter, the entire shelf cooled with respect to the mean SST (Fig. 2b). However, the shallow areas of the RDP and, mainly, the ER cooled more than the MSF region and much more than the SMG and PVF. At the ER the cooling results of 4.4 °C lower than at the PVF. Conversely, in summer the entire shelf heated with respect to the mean SST (Fig. 2b), but the shallow waters heated more than the adjacent waters and the middle shelf, and much more (around 4 °C) than the SMG and PVF.

Mode 2 reveals the different heating and cooling that take place in the intermediate seasons, which can hardly be appreciated in previous figures. Mode 2 significant cases corresponded to early spring and early fall (September and April; Fig. 6c and 6d, respectively) in the positive (with 39 days) and negative (with 35 days) phases of the mode, respectively. In early spring, the

region comprised between the 10 m and 60 m isobaths showed a temperature increment of around 3 °C, while the temperatures at RDP, SMG, and the inner ER increased less than 2 °C. In the fall, SST cooling was more pronounced in ER and the MSF areas, where a decreased of more than 4 °C was observed and minimizes in middle and internal RDP, western ER, and SMG.

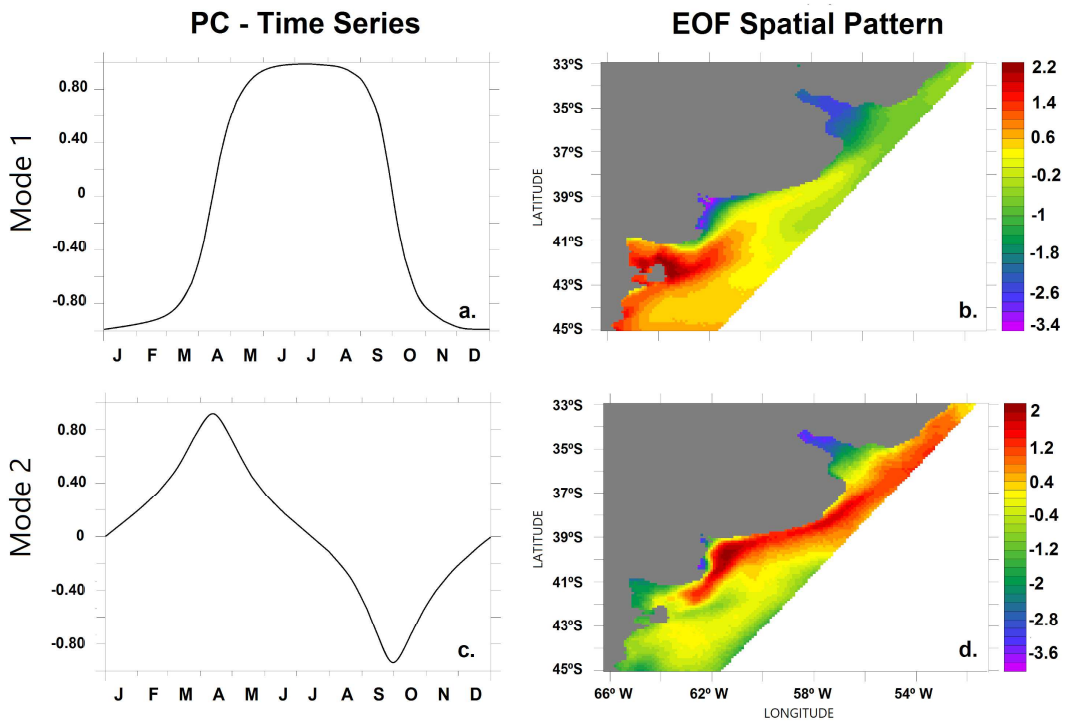

.

Figure 5. Average principal component associated with the Mode 1 (a., accounting 70% of the variance) and Mode 2 (c., 24% of the variance) of SST seasonal variability in the NACS, showing the monthly correlation between each mode and the SST field. EOF spatial structure associated with Mode 1 (b.) is mainly related to Areas I and II occurring in late spring and summer (Oct-Mar), and in late autumn and winter (May-Sep); while the associated with Mode 2 (d.) occurs in Area III with maximum negative values in spring (Sep-Oct) and positive values in autumn (Mar-May).
Figura 5. Componentes principales (series temporales) asociadas al Modo 1 (a., 70% de la varianza) y al Modo 2 (c., 24% de la varianza) de variabilidad de TSM en la Plataforma Continental Argentina Norte, mostrando la correlación mensual entre cada modo y el campo de TSM. La estructura EOF espacial asociada con el Modo 1 (b.) está principalmente relacionada a las Áreas I y II que ocurren en la primavera temprana y verano (oct-mar), y en otoño tardío e invierno (may-sep); mientras que la estructura asociada al Modo 2 (d.) ocurre en el Área III con valores máximos negativos en primavera (septiembre y octubre) y valores positivos en otoño (mar-may).

DISCUSSION AND CONCLUSIONS

Twelve years of daily satellite data were used to describe SST seasonal variability at seasonal timescales in the NACS. An accurate definition of the seasonal cycle was utilized, computed as a harmonic analysis that extracts the annual and semi-annual components, and statistical techniques were applied to show the principal modes of variability in this spatial scale. Our results update and improve the knowledge of the SST seasonal cycle in the NACS.

SST annual variability accounted over 90% of the total variance analysis in the NACS, with the highest values (>96%) in ER. This variability was related to the forcing mechanisms associated with the seasonal fluctuations in the solar radiation received by the ocean surface, which has an approximately sinusoidal signature (Seckel and Beaudry, 1973).

Annual mean SST in the NACS ranged between 10.5 and 20 °C. The highest temperatures were found in the northern shelf and the lowest values over the southern part, with isotherms following in coincidence the shelf isobathic features, as a result of a combination of the regional circulation and the net surface heat flux. Strong currents driven by the dominant semidiurnal tide

(M_2) inhibit the formation of the seasonal thermocline in some coastal areas of the Patagonian shelf, inducing homogenization of the whole water column even during the spring and summer when the surface heat flux increases (Glorioso, 1987; Pisoni et al., 2015; Rivas et al., 2006; Rivas, 2010). In our results, an isolated low temperature cell was observed in PVF region, as a unique feature associated with the dynamic of this tidal front, where vertical mixing tends to damp the seasonal heating/cooling.

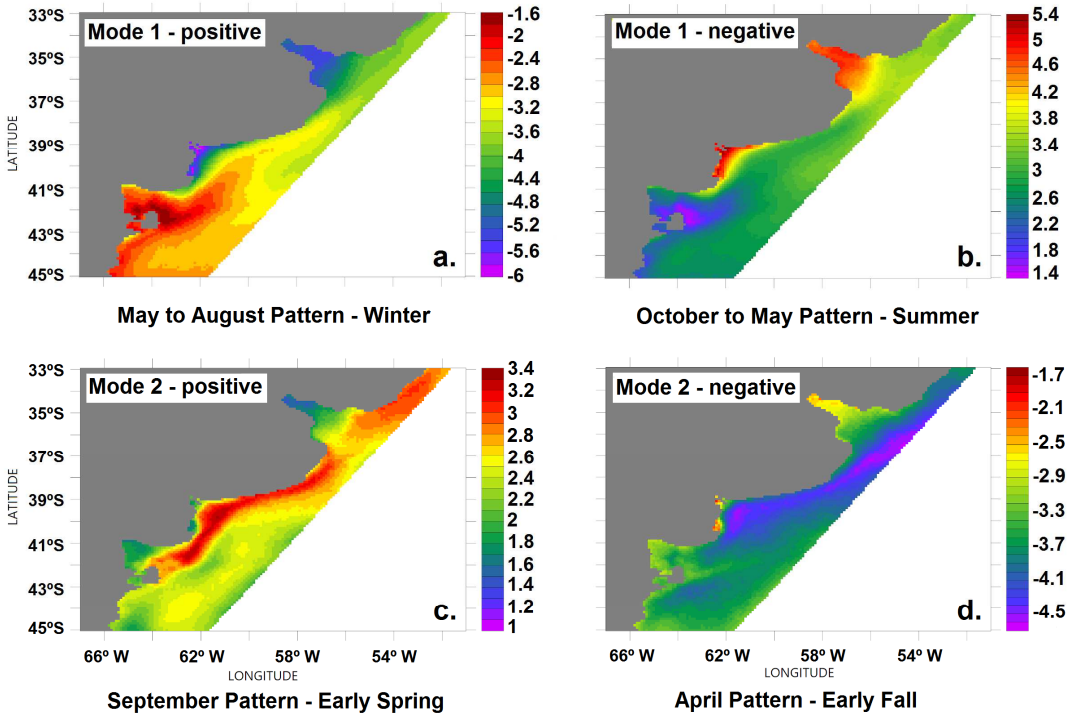

.

Figure 6. Composites of the SST (°C) fields associated with the Mode 1 (upper panels) and the Mode 2 (lower panels) of annual variability in its positive (a. and c.) and negative (b. and d.) phases for the Northern Argentinean Continental Shelf. Note that the scale of every figure is different.
Figura 6. Campos de composiciones de SST (°C) asociados con el Modo 1 (paneles superiores) y el Modo 2 (paneles inferiores) de variabilidad anual y sus fases positivas (a. y c.) y negativas (b. y d.) para la Plataforma Continental Argentina Norte. Notar que la escala de colores de cada figura es diferente.

Monthly mean SST spatial distribution associated with the seasonal cycle showed a SST gradient pointing in the northwest direction (onshore) in most areas all year round, remarking that shallow areas heat/cool rapidly as seasons change. Minimum SSTs occur in August and maximum SSTs in February, in agreement with other studies for different parts of our study area (*e.g.*, Hoffman et al., 1997; Lentini et al., 2000; Martínez-Avellaneda, 2005; Podestá et al., 1991).

The spatial distribution of SST variance, its annual cycle amplitude and phase could be associated with water response to changes in the radiative cycle and allowed us to define three main areas with particular behaviors:

- **Area I**: the inner regions of ER and RDP, with depth less than 20 m, that showed the highest amplitudes, with differences over 6.8 °C between the warm and cold seasons, and the highest phases (>60 days);
- **Area II**: the SMG and shelf water around PVF where the lowest amplitudes (less than 4.6 °C) and phases (less than 40 days) occurred;
- **Area III**: the middle coastal shelf water that "connects" or "involves" the previous areas, associated with MSF dynamics.

The amplitude of the annual cycle showed values from 7.6 °C to 3.4 °C; this result is lower than that previously obtained for the whole NACS by Podestá et al. (1991) and equal or somewhat higher than that obtained by Rivas (2010). The annual cycle phase (days from July 27th where SST annual cycle reaches its minimum) showed that first cycle's minimum in the

RDP and ER areas was around day 70 (October 5th), while the shelf and in offshore waters got it around day 40 (September 5th, *i.e.*, one month before), and, as noted by Podestá et al., (1991), the PVF area showed lower values, around day 30 (August 26th).

The near north-south differences north of 41º S shown by these results suggested a predominantly astronomical forcing, *i.e.,* solar radiation, of the SST annual cycle. The decrease in amplitude and phase with higher depth could be associated with slower water response to changes in the radiative cycle due to higher depth or due to vertical mixing, as a result of wind and tides, which distributes heat throughout the water column (Glorioso, 1987) diluting the effect of the radiative cycle. The amplitude is lower in areas that do not show seasonal stratification, such as PVF, and where summer heat flux is distributed over the whole water column (Rivas 2010). The semi-annual cycle amplitude (not shown) resulted very small (< 1 °C) at the inner shelf and the coastal areas; consistently, it is known that this cycle is mostly related to the system of the SWAO boundary currents (Goñi et al., 2011; Provost et al., 1992) which is out of the scope of this work.

The dominant EOF mode of SSTA (Mode 1, accounting for 70% of the variance) was mainly related to ER and RDP inner water (Area I) and SMG and PVF water (Area II), and was more intense (higher score values) in late spring and summer (October to March) and in late autumn and winter (May to September), reflecting the effect of the annual radiative cycle. As the cold season progresses, the shallow waters of ER and the RDP (Area I) cool faster than the deeper waters of the shelf and the SMG/PVF regions (Area II). As a result, during late autumn/winter those shallow regions become colder than the deeper ones and the temperature gradient points southward and offshore, getting temperatures ~ 3 °C lower than the adjacent waters and the middle shelf, and ~ 4 °C lower than the SMG and PVF. Reciprocally, during late spring/summer, the Area I heat faster than the north middle shelf (~ 2 °C hotter), SMG and the Patagonian coastal shelf (more than ~ 3.5 °C hotter) and, therefore, the temperature gradient points northward and onshore. Although the Area III (middle region, MSF) had similar amplitude and phase, this Mode 1 allow us to differentiate it around 38° S.

The second EOF mode (accounting for 24% of the variance) was mainly associated with the middle shelf water and MSF (Area III) and showed more intensity during early spring (September-October, negative phase) and early autumn (March-May, positive phase). It showed a pattern where SSTA gradient pointing offshore suggest the heating/cooling of coastal waters feature. This mode could be related to a transition at the early intermediate seasons when this heating/cooling extends along the coastal region between PVF and RDP, and surface heat and freshwater fluxes get maximum extreme values (Scasso and Piola, 1988). In early spring, the region comprehended between 20-60 m isobaths showed a 3-3.4 °C temperature increment, whereas the RDP, SGM, and the inner ER got less than 2.2 °C heating. In early fall, SST cooling was stronger in ER and the MSF area where it got a 4-4.7 °C decrease and minimized in middle and internal RDP, western ER, and SMG. The mean circulation of coastal shelf waters over the NACS is from the SSW to the NNE, and following the bathymetry (Severov, 1990; Piola and Rivas, 1997; Guerrero and Piola, 1997). Across the central portion of the NACS, the NNE direction of the flow prevails throughout the year, as it can be inferred from the salinity distributions in Lucas et al. (2005). Waters exported from the SMG cover almost the whole area between the coast and the 50-m isobath and show large seasonal variation in extent and distribution (Lucas et al., 2005). During the winter months, the entire area off ER is dominated by the northward extension of the SMG waters. In the spring-summer period, the retraction of SMG waters in the ER area appears to allow the expansion of the ER estuarine low salinity signal along the coast and to the east, an effect enhanced by the formation of a southward coastal flow of shelf waters during this season proposed by Palma et al., 2004b.

While flowing towards lower latitudes, the continental shelf water is subject to an excess of evaporation over precipitation (Scasso and Piola, 1988), thus increasing the salinity along its path over Area III. The excess of evaporation implies an exchange of net heat with the atmosphere through latent heat flux, as the process of evaporation will absorb heat from the surrounding waters, thus implying cooler SSTs. The net air-sea exchange of water in the SMG area shows similar seasonality as the evaporation rate (*i.e.*, with a minimum in September and a maximum in the fall (Scasso and Piola, 1988)) while the precipitation rate is nearly constant throughout the year. As the difference between evaporation and precipitation is always positive, there is net loss of water to the atmosphere throughout the year (Scasso and Piola, 1988). Over this region, Mode 2 indicates warm SSTA in the spring and cool SSTA in the fall (Fig. 6).

Therefore, the Mode 2 suggests the presence of a warm water mass in an area where evaporation exceeds the precipitation rate. Minimum evaporation rates in September / Spring

suggests less ocean heat loss, and thus, warmer SSTs (*i.e.*, positive SSTA). Whereas in the fall, the SMG water begin to cover the ER area and the excess of evaporation is at its peak, thus, the loss of heat through latent heat flux is greater, resulting in cooler SSTs (*i.e.*, negative SSTA).

This study showed the importance of seasonal cycle on NACS hydrographic conditions and defined three main areas with similar SST behavior. It denoted that within the RDP and ER region there are at least two areas with different amplitude and phase of variation. Computing the timing of the annual cycle can be useful to comprehend the occurrence, distribution and migration of local economic fish stocks, which could explain the variation in temporal availability of preferred habitat for, for example, cold water species along the coast (*e.g.*, *Discopyge tschuddi*, Cortés et al., 2011). Therefore, the variability of SST condition would not only determine the species/stage vulnerability (Jaureguizar et al., 2007, 2015, 2016; Jaureguizar and Guerrero, 2009) during evaluation cruises or fishery, affecting estimates of densities (sub/overestimation) and fishery mortality, and have implications in management regulations of fish stocks, but also affects the reproductive potential (Elisio et al., 2017; Militelli, 2007), species recruitment (Marrari et al., 2013), and affect the ratio of consumption over biomass (Q/B) within the NACS (Lercari et al., 2018, in press) and would therefore have serious implications for the sustainability of the ecosystem.

Acknowledgements: This paper is a contribution to the ANPCyT (National Agency for Scientific and Technological Research of Argentina) PICT 2014-2672 and 2015-1934 Projects; UBACYT 20020150100118BA (Universidad de Buenos Aires) and PIDDEF 2014 N°14 (Ministerio de Defensa, Secretaría de Ciencia, Tecnología y Producción para la Defensa, Subsecretaría de Investigación, Desarrollo y Producción para la Defensa, Programa de Investigación y Desarrollo para la Defensa). Dr. Luz Clara and Dr. Simionato's salaries were paid by the CONICET. Dr. Jaureguizar's salary was paid by the CIC-Provincia de Buenos Aires. The authors are grateful to Reviewer H for his/her careful reading of the manuscript and constructive comments and suggestions to significantly improve the explanation of the methodological work, as well as Dr. R.A. Maenza for his constructive critical reading. INIDEP contribution #2178.

REFERENCES

Acha, E. M., Mianzan, H. W., Guerrero, R. A., Favero, M., y Bava, J. (2004). Marine fronts at the continental shelves of austral South America. *Journal of Marine Systems*, *44*(1–2), 83–105. doi: 10.1016/j.jmarsys.2003.09.005

Bava, J., Gagliardini, D. A., Dogliotti, A. I. y Lasta, C. A. (April 8-12, 2002). Annual distribution and variability of remotely sensed sea surface temperature fronts in the Southwestern Atlantic Ocean. 29th International Symposium on Remote Sensing of Environment, Com. Nac. de Activ. Espaciales, Buenos Aires, Argentina.

Bianchi, A. A. (2005). Vertical stratification and air-sea CO2 fluxes in the Patagonian shelf. Journal of Geophysical Research, 110(C7), C07003. doi: 10.1029/2004JC002488

Bianchi, A. A., Pino, D. R., Perlender, H. G. I., Osiroff, A. P., Segura, V., Lutz, V., … Piola, A. R. (2009). Annual balance and seasonal variability of sea-air CO 2 fluxes in the Patagonia Sea: Their relationship with fronts and chlorophyll distribution. Journal of Geophysical Research, 114(C3), C03018. doi: 10.1029/2008JC004854

Carreto, J. I., Benavides, H. R., Negri, R. M., y Glorioso, P. D. (1986). Toxic red-tide in the Argentine Sea. Phytoplankton distribution and survival of the toxic dinoflagellate *Gonyaulax excavata* in a frontal area. *Journal of Plankton Research*, *8*(1), 15–28. doi: 10.1093/plankt/8.1.15

Carreto, Josél., A. Lutz, V., Carignan, M. O., Cucchi Colleoni, A. D., y De Marco, S. G. (1995). Hydrography and chlorophyll a in a transect from the coast to the shelf-break in the Argentinian Sea. *Continental Shelf Research*, *15*(2–3), 315–336. doi: 10.1016/0278-4343(94)E0001-3

Cortés, F., Jaureguizar, A. J., Menni, R. C., y Guerrero, R. A. (2011). Ontogenetic habitat preferences of the narrownose smooth-hound shark, Mustelus schmitti, in two Southwestern Atlantic coastal areas. *Hydrobiologia*, *661*(1), 445–456. doi: 10.1007/s10750-010-0559-2

De Wysiecki, A. M., Jaureguizar, A. J., y Cortés, F. (2017). The importance of environmental drivers on the narrownose smoothhound shark (Mustelus schmitti) yield in a small-scale gillnet fishery along the southern boundary of the Río de la Plata estuarine area. *Fisheries Research*, *186*, 345–355. doi: 10.1016/j.fishres.2016.10.011

Delgado, A. L., Jamet, C., Loisel, H., Vantrepotte, V., Perillo, G. M. E., y Piccolo, M. C. (2014). Evaluation of the MODIS-Aqua Sea-Surface Temperature product in the inner and mid-shelves of southwest Buenos Aires Province, Argentina. *International Journal of Remote Sensing*, *35*(1), 306–320. doi: 10.1080/01431161.2013.870680

Derisio, C., Alemany, D., Acha, E. M., y Mianzan, H. (2014). Influence of a tidal front on zooplankton abundance, assemblages and life histories in Península Valdés, Argentina. *Journal of Marine Systems*, *139*, 475–482. doi: 10.1016/j.jmarsys.2014.08.019

Deser, C., Alexander, M. A., Xie, S.-P., y Phillips, A. S. (2010). Sea Surface Temperature Variability: Patterns and Mechanisms. *Annual Review of Marine Science*, *2*(1), 115–143. doi: 10.1146/annurev-marine-120408-151453

Elisio, M., Colonello, J. H., Cortés, F., Jaureguizar, A. J., Somoza, G. M., y Macchi, G. J. (2017). Aggregations and reproductive events of the narrownose smooth-hound shark (Mustelus schmitti) in relation to temperature and depth in coastal waters of the south-western Atlantic Ocean (38–42°S). *Marine and Freshwater Research*, *68*(4), 732. doi: 10.1071/MF15253

Framiñan, M. B., Etala, M. P., Acha, E. M., Guerrero, R. A., Lasta, C. A., y Brown, O. B. (1999). Physical Characteristics and Processes of the Río de la Plata Estuary. In G. M. E. Perillo, M. C. Piccolo, y M. Pino-Quivira (Eds.), *Estuaries of South America* (pp. 161–194). doi: 10.1007/978-3-642-60131-6_8

Garcia, C. A. E., y Garcia, V. M. T. (2008). Variability of chlorophyll-a from ocean color images in the La Plata continental shelf region. *Continental Shelf Research*, *28*(13), 1568–1578. doi: 10.1016/j.csr.2007.08.010

Giese, B. S. y Carton, J. A. (1994). The Seasonal Cycle in Coupled Ocean-Atmosphere Model. *Journal of Climate*, *7*, 1208–1217.

Glorioso, P. D. (1987). Temperature distribution related to shelf-sea fronts on the Patagonian Shelf. *Continental Shelf Research*, *7*(1), 27–34. doi: 10.1016/0278-4343(87)90061-6

Glorioso, P. D., y Flather, R. A. (1997). The Patagonian Shelf tides. *Progress in Oceanography*, *40*(1–4), 263–283. doi: 10.1016/S0079-6611(98)00004-4

Goni, G. J., Bringas, F., y DiNezio, P. N. (2011). Observed low frequency variability of the Brazil Current front. *Journal of Geophysical Research*, *116*(C10), C10037. doi: 10.1029/2011JC007198

Guerrero, R. A. y Piola, A. R. (1997). Masas de agua en la plataforma continental. In E. Boschi. (Ed.), *El Mar Argentino y sus Recursos Pesqueros, Tomo I: Antecedentes Históricos de las Exploraciones en el Mar y las Características Ambientales* (pp. 107–119). Bahía Blanca, Argentina: Instituto Nacional de Investigación y Desarrollo Pesquero.

Guerrero, R. A. (1998). Oceanografía física del estuario del Río de la Plata y el sistema costero de El Rincón. In C. A. Lasta, (Ed.), *Resultados de una campaña de evaluación de recursos demersales costeros de la Provincia de Buenos Aires y del litoral uruguayo.* INIDEP Informe Técnico Nº 8, 21 (pp. 29–54). Mar del Plata, Argentina.

Hannachi A. (2004). A Primer for EOF Analysis of Climate Data. Department of Meteorology, University of Reading, Reading, U.K.

Hoffman, J. A. J., Núñez M. N., y Piccolo, M. C. (1997). Características Climáticas del Atlántico Sudoccidental. In E. Boschi, (Ed.), *El Mar Argentino y sus Recursos Pesqueros: 1* (pp. 163– 193). Mar del Plata, Argentina: Inst. Nac. De Investigación y Desarrollo Pesquero.

Jaureguizar, A. J., y Raúl, G. (2009). Striped weakfish (Cynoscion guatucupa) population structure in waters adjacent to Rio de la Plata, environmental influence on its inter-annual variability. *Estuarine, Coastal and Shelf Science*, *85*(1), 89–96. doi: 10.1016/j.ecss.2009.04.013

Jaureguizar, A. J., Solari, A., Cortés, F., Milessi, A. C., Militelli, M. I., Camiolo, M. D., … García, M. (2016). Fish diversity in the Río de la Plata and adjacent waters: An overview of environmental influences on its spatial and temporal structure: environment influence on fish diversity of río de la plata. *Journal of Fish Biology*, *89*(1), 569–600. doi: 10.1111/jfb.12975

Jaureguizar, A. J., Cortés, F., Milessi, A. C., Cozzolino, E., y Allega, L. (2015). A trans-ecosystem fishery: Environmental effects on the small-scale gillnet fishery along the Río

de la Plata boundary. *Estuarine, Coastal and Shelf Science*, *166*, 92–104. doi: 10.1016/j.ecss.2014.11.003

Jaureguizar, A. J., Waessle, J. A., y Guerrero, R. A. (2007). Spatio-temporal distribution of Atlantic searobins (Prionotus spp.) in relation to estuarine dynamics (Río de la Plata, Southwestern Atlantic Coastal System). *Estuarine, Coastal and Shelf Science*, *73*(1–2), 30–42. doi: 10.1016/j.ecss.2006.12.012

Kara, A. B., Wallcraft, A. J., Hurlburt, H. E., y Loh, W.-Y. (2009). Which surface atmospheric variable drives the seasonal cycle of sea surface temperature over the global ocean? *Journal of Geophysical Research*, *114*(D5), D05101. doi: 10.1029/2008JD010420

Lentini, C. A. D., Campos, E. J. D., y Podestá, G. G. (2000). The annual cycle of satellite derived sea surface temperature on the western South Atlantic shelf. *Revista Brasileira de Oceanografia*, *48*(2), 93–105. doi: 10.1590/S1413-77392000000200001

Lercari, D., Milessi, A. C., Vögler, R., Velasco, G., y Jaureguizar, A. J. (2018). Modelos tróficos en el Atlántico Sud Occidental: evaluando la estructura y funcionamiento de ecosistemas costeros. In P. Muniz, D. Conde, N. Venturini, E. Brugnoli. (Eds.), *Ciencias Marino Costeras en el Umbral del Siglo XXI: Desafíos en Latinoamerica y el Caribe.* XV COLACMAR. Sección: Estructura y Funcionamiento de Comunidades y Ecosistemas Marino-Costeros. Punta del Este, Uruguay.

Lucas, A. J., Guerrero, R. A., Mianzán, H. W., Acha, E. M., y Lasta, C. A. (2005). Coastal oceanographic regimes of the Northern Argentine Continental Shelf (34–43°S). *Estuarine, Coastal and Shelf Science*, *65*(3), 405–420. doi: 10.1016/j.ecss.2005.06.015

Lutz, V. A., Segura, V., Dogliotti, A. I., Gagliardini, D. A., Bianchi, A. A., y Balestrini, C. F. (2010). Primary production in the Argentine Sea during spring estimated by field and satellite models. *Journal of Plankton Research*, *32*(2), 181–195. doi: 10.1093/plankt/fbp117

Marrari, M., Signorini, S. R., McClain, C. R., Pájaro, M., Martos, P., Viñas, M. D., … Buratti, C. (2013). Reproductive success of the Argentine anchovy, *Engraulis anchoita* , in relation to environmental variability at a mid-shelf front (Southwestern Atlantic Ocean). *Fisheries Oceanography*, *22*(3), 247–261. doi: 10.1111/fog.12019

Martínez Avellaneda, N. (2005). *Ciclo Anual y Variabilidad de baja frecuencia de la Temperatura Superficial del Mar en el Océano Atlántico Sudoccidental* (Tesis de Licenciatura en Oceanografía). Universidad de Buenos Aires, Facultad de Ciencias Exactas y Naturales, Buenos Aires, Argentina.

Martos, P., y Piccolo, M. C. (1988). Hydrography of the Argentine continental shelf between 38° and 42°S. *Continental Shelf Research*, *8*(9), 1043–1056. doi: 10.1016/0278-4343(88)90038-6

Meccia, V. L., Simionato, C. G., Fiore, M. E., D'Onofrio, E. E., y Dragani, W. C. (2009). Sea surface height variability in the Rio de la Plata estuary from synoptic to inter-annual scales: Results of numerical simulations. *Estuarine, Coastal and Shelf Science*, *85*(2), 327–343. doi: 10.1016/j.ecss.2009.08.024

Menni, R. C., Jaureguizar, A. J., Stehmann, M. F. W., y Lucifora, L. O. (2010). Marine biodiversity at the community level: Zoogeography of sharks, skates, rays and chimaeras in the southwestern Atlantic. *Biodiversity and Conservation*, *19*(3), 775–796. doi: 10.1007/s10531-009-9734-z

Militelli, M. I. (2007). *Biología reproductiva comparada de especies de la familia Sciaenidae en aguas del Río de la Plata y Costa Bonaerense* (Tesis Doctoral). Universidad Nacional de Mar del Plata, Facultad de Ciencias Exactas y Naturales, Mar del Plata, Argentina.

Moreira, D., Simionato, G. G., y Dragani, W. (*2011*). Modeling Ocean Tides and Their Energetics in the North Patagonia Gulfs of Argentina. (2011). *Journal of Coastal Research*, *27*(1), 87. doi: 10.2112/JCOASTRES-D-09-00055.1

North, G. R., Bell, T.L., Cahalan, R. F., y Moeng, F. J. (1982). Sampling errors in the estimation of empirical orthogonal functions. *Mon. Weather Rev.*, *110*, 699–706.

Palma, E. D. (2004). A comparison of the circulation patterns over the Southwestern Atlantic Shelf driven by different wind stress climatologies. *Geophysical Research Letters*, *31*(24), L24303. doi: 10.1029/2004GL021068

Palma, E. D., Matano, R. P., y Piola, A. R. (2004b). A numerical study of the Southwestern Atlantic Shelf circulation: Barotropic response to tidal and wind forcing: SOUTHWESTERN ATLANTIC SHELF CIRCULATION. *Journal of Geophysical Research: Oceans*, *109*(C8), n/a-n/a. doi: 10.1029/2004JC002315

Palma, E. D., Matano, R. P., y Piola, A. R. (2008). A numerical study of the Southwestern Atlantic Shelf circulation: Stratified ocean response to local and offshore forcing. *Journal of Geophysical Research*, *113*(C11), C11010. doi: 10.1029/2007JC004720

Parker, G., Paterlini M. C. y Violante, R. A. (1997). El fondo marino. In E. Boschi. *El Mar Argentino y sus Recursos Pesqueros, Antecedentes Históricos de las Exploraciones en el Mar y las Características Ambientales, vol. 1* (pp. 65–87). Instituto Nacional de Investigación y Desarrollo Pesquero (INIDEP), Mar del Plata, Argentina.

Piola, A. R. y A. L. Rivas. (1997). Corrientes en la plataforma continental. In E. Boschi. (Ed.), *El Mar Argentino y sus Recursos Pesquero, Tomo I: Antecedentes históricos de las exploraciones en el mar y las características ambientales* (pp. 119–132). Instituto Nacional de Investigación y Desarrollo Pesquero, Mar del Plata, Argentina.

Piola, A. R. y Scasso, L. M. (1988). Circulación en el Golfo San Matías. *Geoacta, 15*(1), 33–51.

Pisoni, J. P., Rivas, A. L., y Piola, A. R. (2015). On the variability of tidal fronts on a macrotidal continental shelf, Northern Patagonia, Argentina. *Deep Sea Research Part II: Topical Studies in Oceanography*, *119*, 61–68. doi: 10.1016/j.dsr2.2014.01.019

Podestá G. P., Brown O. B., y Evans, R. H. (1991). The annual cycle of satellite-derived sea surface temperature in the Southwestern Atlantic Ocean. *American Meteorological Society, Journal of Climate*, *4*, 157-467. doi: 10.1175/1520-0442(1991)004<0457:TACOSD>2.0.CO;2

Powell, B. S., Arango, H. G., Moore, A. M., Di Lorenzo, E., Milliff, R. F., y Foley, D. (2008). 4DVAR data assimilation in the Intra-Americas Sea with the Regional Ocean Modeling System (ROMS). *Ocean Modelling*, *23*(3–4), 130–145. doi: 10.1016/j.ocemod.2008.04.008

Provost, C., Garcia, O., y Garçon, V. (1992). Analysis of satellite sea surface temperature time series in the Brazil-Malvinas Current Confluence region: Dominance of the annual and semiannual periods. *Journal of Geophysical Research: Oceans*, *97*(C11), 17841–17858. doi: 10.1029/92JC01693

Reynolds, R. W., Rayner, N. A., Smith, T. M., Stokes, D. C. y Wang, W. (2002). An improved in situ and satellite SST analysis for climate. *Journal of Climate*, *15*, 1609–1625. *doi: 10.1175/1520-0442(2002)015<1609:AIISAS>2.0.CO;2*

Rivas, A. L. (2010). Spatial and temporal variability of satellite-derived sea surface temperature in the southwestern Atlantic Ocean. *Continental Shelf Research*, *30*(7), 752–760. doi: 10.1016/j.csr.2010.01.009

Rivas, A. L., y Beier, E. J. (1990). Temperature and salinity fields in the nortpatagonic gulfs. *Oceanologica Acta*, *13*, 15–20.

Rivas, A. L., y Pisoni, J. P. (2010). Identification, characteristics and seasonal evolution of surface thermal fronts in the Argentinean Continental Shelf. *Journal of Marine Systems*, *79*(1–2), 134–143. doi: 10.1016/j.jmarsys.2009.07.008

Rivas, A. L., Dogliotti, A. I., y Gagliardini, D. A. (2006). Seasonal variability in satellite-measured surface chlorophyll in the Patagonian Shelf. *Continental Shelf Research*, *26*(6), 703–720. doi: 10.1016/j.csr.2006.01.013

Saraceno, M. (2004). Brazil Malvinas Frontal System as seen from 9 years of advanced very high resolution radiometer data. *Journal of Geophysical Research*, *109*(C5), C05027. doi: 10.1029/2003JC002127

Scasso, L., y Piola, A. (1988). Intercambio neto de agua entre el mar y la atmósfera en el Golfo San Matías. *Oceanologica Acta*, *15*(1): 13-31.

Seckel, G. R. y Beaudry, F. H. (1973). *The radiation from sun and sky over the North Pacific Ocean*. *Trans. Amer. Geophys. Union*, *54*, 1114.

Severov, D. N. (1990). Particularidades de las condiciones oceanológicas del Atlántico Sud-occidental sobre la base de características temporales medias procedentes de una serie de años. *Frente Marítimo*, *6*, 109–119.

Shiklomanov, I. (1998). *World Water Resources-A new appraisal and assessment for the 21st. century*. París, France: UNESCO.

Simionato, C. G., Clara Tejedor, M. L., Campetella, C., Guerrero, R., y Moreira, D. (2010). Patterns of sea surface temperature variability on seasonal to sub-annual scales at and offshore the Río de la Plata estuary. *Continental Shelf Research*, *30*(19), 1983–1997. doi: 10.1016/j.csr.2010.09.012

Simionato, C. G., Vera, C. S., y Siegismund, F. (2005). Surface Wind Variability on Seasonal and Interannual Scales Over Río de la Plata Area. *Journal of Coastal Research*, *214*, 770–783. doi: 10.2112/008-NIS.1

Simionato, C. G., Nuñez, M. N., y Engel, M. (2001). The salinity front of the Río de la Plata—A numerical case study for winter and summer conditions. *Geophysical Research Letters*, *28*(13), 2641–2644. doi: 10.1029/2000GL012478

Trenberth, K. E., y Stepaniak, D. P. (2004). The flow of energy through the earth's climate system. *Quarterly Journal of the Royal Meteorological Society*, *130*(603), 2677–2701. doi: 10.1256/qj.04.83

von Storch, H., y Zwiers, F. W. (1999). *Statistical Analysis in Climate Research*. Cambridge, UK: Cambridge Univ. Press.

Wang, C., Xie, S. P., y Carton, J. A. (Eds.). (2004). *Earth's Climate: The Ocean-Atmosphere Interaction*. doi: 10.1029/GM147

Wick, G. A., Jackson, D. L., y Castro, S. L. (2004). Production of an enhanced blended infrared and microwave sea surface temperature product. *IEEE International IEEE International IEEE International Geoscience and Remote Sensing Symposium, 2004. IGARSS '04. Proceedings. 2004*, *2*, 835–838. doi: 10.1109/IGARSS.2004.1368534

Yashayaev, I. M., y Zveryaev, I. I. (2001). Climate of the seasonal cycle in the North Pacific and the North Atlantic oceans. *International Journal of Climatology*, *21*(4), 401–417. doi: 10.1002/joc.585

Recibido: Marzo, 2018
Aceptado: Junio, 2019